Removal of Ocular Artifacts with the Utilization of Filter Banks

Umut Orhan[1,2(✉)] and Santosh Mathan[1]

[1] Honeywell Laboratories, Redmond, WA, USA
[2] Cortech LLC, Atlanta, GA, USA
umut.orhan@honeywell.com

Abstract. Eye blinks and other ocular artifacts represent a dominant source of EEG signal interference, especially in frontal EEG electrodes. Even though there are several widely accepted methods for the removal eye-blinks, (e.g. linear filtering and ICA), it is still a difficult problem to address when the number of EEG electrodes are limited (as is the case for EEG systems designed for everyday application contexts), and dedicating a subset of these for monitoring eye activity is impractical. In this paper, we propose a novel and general method to eliminate the ocular artifacts based on a combination of filter banks and an eye tracker. This approach offers the promise of making non-intrusive, efficient, and robust ocular artifact detection and correction a tractable prospect.

Keywords: Artifacts · EEG · Ocular · Filter banks · Filtering

1 Introduction

Accurate estimation of mental workload is a capability of considerable theoretical and practical interest. Applications include estimating learning efficiency, assessing cognitive deficiencies, and serving as the basis for adapting human computer interfaces [1,2]. Inferences of cognitive load are typically made by assessing task performance related metrics, behavioral actions and measurement of various physiological signals like eye activity, heart rate or electroencephalography (EEG). EEG, as a measure of ongoing cortical activity, offers the prospect of direct, quantitative assessment of workload. However these signals can be compromised by artifacts and interferences, consequently decreasing the robustness and reliability of the estimation of the cognitive state. In particular, cognitive tasks requiring eye movements increase the likelihood of ocular artifacts. Eye blinks constitute one of the most prominent artifact sources due to their relatively large amplitude in EEG compared to the neural activity. Even though the removal of ocular artifacts has been widely addressed [3–7], effective filtering when only a low number of EEG electrodes are available, and when a dedicated electrooculogram (EOG) impractical, is still an important and interesting problem.

In this paper, we address the problem of the correction of ocular artifacts in EEG using filter banks, with the joint utilization of an eye tracker as the

D.D. Schmorrow and C.M. Fidopiastis (Eds.): AC 2015, LNAI 9183, pp. 504–513, 2015.
DOI: 10.1007/978-3-319-20816-9_48

basis for accurate and robust correction of eye artifacts. Reliance on a combination of EEG, and eye tracker data requires an additional consideration of the synchronization of the signals, which is typically underestimated or ignored in the literature. Therefore, we first illustrate the importance of the signal synchronization and demonstrate a procedure to achieve event matching and signal resampling. Consequently, we introduce a filter bank based artifact removal, which is the main novelty of this paper. Even though the proposed methodology is specifically designed for the removal of (EOG) artifacts, these methods are generalizable to other artifact sources with sufficient ease.

2 Methods

2.1 Signal Synchronization

For the joint utilization of two or more independently recorded discrete signal sources, it is imperative to synchronize the corresponding sample times. This importance is primarily a consequence of the slight differences between actual sampling rates and nominal sampling rates. These small discrepencies stem from the practicality of the recording hardware or rounded reporting of the nominal sampling rates. For example, the characteristics of oscillators used for analog to digital conversion in most recording equipment depends on temperature, causing slight deviations from the tuning frequency. Even the slightest difference between the nominal and actual sampling rates might become relatively significant over the span of minutes. To illustrate this phenomenon, let T, f_n and f_s be the recording duration, nominal sampling rate and actual sampling rate, respectively. Corresponding time difference introduced at the end of the recording due to the sampling rate difference becomes,

$$\Delta t = T \left| 1 - \frac{f_s}{f_n} \right| .$$

For $T = 20\,\text{min}$, $f_s = 59.99\,\text{Hz}$ and $f_n = 60\,\text{Hz}$, Δt becomes 200 ms, which might be extremely significant for a psychological experiment or for time-locked EEG analysis. Additionally, some of the recording equipment might contain discontinuities due to data losses or exclusions, which contributes further to signal synchronization problems. For example, an eye tracker may stop recording after prolonged durations of looking away.

Event Matching. Event synchronization between the recording equipments can be addressed by utilization of shared hardware triggers. The experimental stimulus or task computer may send simultaneous trigger events to all devices. To align the independently recorded triggers, common event sequences may be matched iteratively, starting from the longest one and removing the matched event sequences. This longest event sequence matching may be solved by the longest common substring problem [8,9], which can be solved in linear time.

Such an event matching approach is only applicable when the event triggers do not contain many repeated sequences.

Following is a high-level operational overview of the simple event matching algorithm, which separates events to blocks according to the matching of the event sequences. Let $e_{k,m}, n_{k,m}$ represent the event label and position pair corresponding to m^{th} event for recording device k,

1. For block v, starting from $v = 0$
2. Find the longest common sequence $s_{v,0}, s_{v,1}, s_{v,2}, \cdots, s_{v,L_v-1}$ over the event labels, where $s_{v,0}$ corresponds to the event pair of $e_{k,m_{k,v}}, n_{k,m_{k,v}}$ for each device k.
3. Remove the event sequence block from the event sequences corresponding to each device.
4. $v = v + 1$

It is worthwhile to note that if there are no event or data losses, the longest common sequence would correspond to the sequence of all the events.

Resampling. Bringing signals to a common sampling rate might be necessary for some signal processing applications. In particular, most adaptive filtering algorithms, e.g. least mean squares (LMS), recursive least squares (RLS) [10], typically expect signals to have identical sampling rates. Even though sample-rate conversion is well-known in discrete time signal processing [11,12], the consideration of the variations from the nominal sampling rates, as indicated in Sect. 2.1, requires additional consideration for their match. Changing the sampling rate by a rational factor, $R = \frac{L}{M}$, may be achieved using the system depicted in Fig. 1, where $\uparrow K$ and $\downarrow K$ represents upsampling and downsampling by a factor of K, respectively.

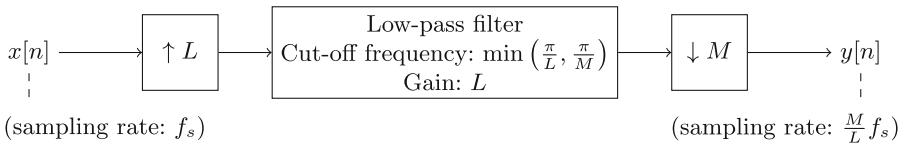

Fig. 1. The system for changing the sampling rate by a factor of $R = \frac{L}{M}$

One of the recording devices is designated as the master device for the purpose of resampling. Correspondingly, a rational common sampling rate is selected relative to the nominal sampling rate of the master device.

For the sake of simplicity, let device 0 be selected as the master device with $f_{n,0}$ as the corresponding nominal sampling rate, and f_c be the common target nominal sampling rate. Subsequently, the sampling rate of device k relative to

the master device in block v may be estimated utilizing the matched events according to

$$Rf_{k,v} = \frac{n_{k,m_{k,v}+L_v-1} - n_{k,m_{k,v}}}{n_{0,m_{0,v}+L_v-1} - n_{0,m_{0,v}}}. \tag{1}$$

Consequently, the corresponding resampling rate becomes,

$$R_{k,v} = Rf_{k,v} \times \frac{f_c}{f_{n,0}}. \tag{2}$$

Accordingly, the signals from device k are resampled by a factor of $R_{k,v}$ for block v (using the resampling system depicted in Fig. 1) to obtain signals synchronized across devices with a nominal sampling rate of f_c. In the following sections, the signals are going to be assumed to have been synchronized.

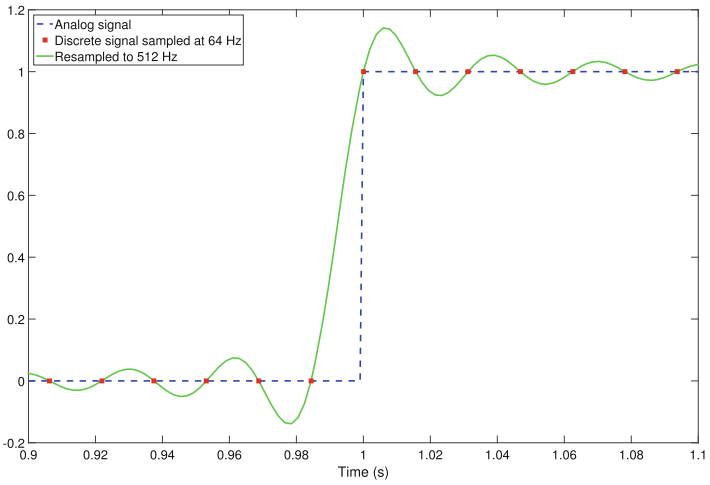

Fig. 2. A demonstration of the ambiguity of the high frequency components. An analog step signal, discrete signal obtained by sampling at 64 Hz and resampled signal obtained by resampling the discrete signal to 512 Hz are all equal at the sampling points.

It is worth noting that the signal synchronization process depicted in this section might have some limitations depending on the content of the signals and events. Expectedly, decreasing the sampling rate would cause high frequency components to be lost. Therefore, if there are signals of interest at high frequencies relative to the corresponding Nyquist rate, the nominal common sampling rate should be set to be sufficiently high. As further consideration, discrete signals do not contain any additional information on their analog counterparts. Typically an anti-aliasing filter is applied prior to analog-to-digital conversion, removing the high frequency components in the analog signal enabling a perfect reconstruction. However, in some contexts, the analog signal might be discontinuous, e.g. step function, correspondingly the resampled signal would be distorted,

since signal is assumed to have zero power beyond the Nyquist frequency. An example of this phenomenon is given in Fig. 2. If this is not the intended behavior for the signals from one of the recording devices, common sampling rate may be selected to be equal to the nominal sampling rate of the corresponding recording device to prevent resampling. Alternatively, if there is more than one such pieces of recording equipment, a specialized resampling method utilizing additional information on the nature of the analog counterpart may be implemented to mitigate the ambiguity of the content beyond the Nyquist frequency.

For the joint utilization of EEG and eye-tracker, the discontinuity mentioned above becomes a matter of concern. When the eye is closed, e.g. during eye blinks, the gaze position or the pupil diameter become untracked for a brief duration. Consequently, the signal is expected to be discontinuous at the time of eye closure or opening. Therefore if the signal of interest in the EEG is negligible beyond the Nyquist rate of the eye tracker, selecting the sampling rate of the eye tracker as the common one would be a reasonable choice. Although the event matching and estimation of the relative sampling rates are sufficient for the algorithm proposed in this paper, we still explored resampling, with the goal of fostering generalizability of the filtering approaches described here.

2.2 Removal of EOG Artifacts

EOG artifacts are typically generated as a consequence of the charge difference caused by the friction of the eyeball during its rotation in the orbit of the eye. Predominantly affecting frontal sites in the EEG, they tend to be relatively large in amplitude compared to the neural activity. Therefore, removal of the EOG artifacts becomes essential for effective brain computer interfaces or cognitive analyses. However, some experimental task paradigms employed might be particularly susceptible to ocular artifacts. For example, an experiment requiring the participant to look at flashing objects at different positions on the monitor may cause considerable ocular interference in the EEG.

In the literature, the methods typically utilized for the removal of ocular artifacts are band-pass filtering, independent component analysis (ICA), principal component analysis (PCA), linear regression and adaptive filtering [4]. These approaches have limitations. For example, since most ocular artifacts tend to be in the lower frequencies, applying a high pass filter may be a useful approach for filtering out artifacts with low impact on the broader EEG spectrum. The main limitation of such a filtering approach is that it is relatively coarse, introducing the possibility of filtering our cortical signals, and leaving residual artifact activity. ICA has been used as a filtering approach as a response to shortcomings associated with high pass filters. Even though ICA or other blind source separation methods are usually effective on identifying eye blinks as an independent source in the EEG without requiring any EOG electrodes or any other external source of indicators, they typically require a high number of EEG channels and manual identification of the interference sources. Moreover, the assumptions of independence and non-Gaussianity in ICA might possibly conflict with the signals of interest or need a substantially large amount of data to be able to identify

the sources [5]. PCA based approaches to artifact corrections have limitations as well. In its characteristic application, PCA maps EEG channels to spatially uncorrelated components. Therefore, PCA inevitably fails to preserve signals of interest occurring in frontal lobes. Linear regression analysis, another commonly used approach to artifact reduction, is typically applied either assuming a proportional propagation of eye activity (measured using EOG sensors placed close to the eye) to EEG channels or matching pre-built templates representing the form of eye blinks. However the variations in the eyeblink shape and possibility of nonlinear progression of eye blinks through scalp limits the effectiveness of regression approaches. Moreover, EOG sensors also pick up neurological activity from frontal lobe. Finally, linear adaptive filters are typically applied with the cost function of minimization of EEG activity, causing possible removal of signal of interest. Additionally, most of the limitations noted for linear regression also apply to linear adaptive filtering.

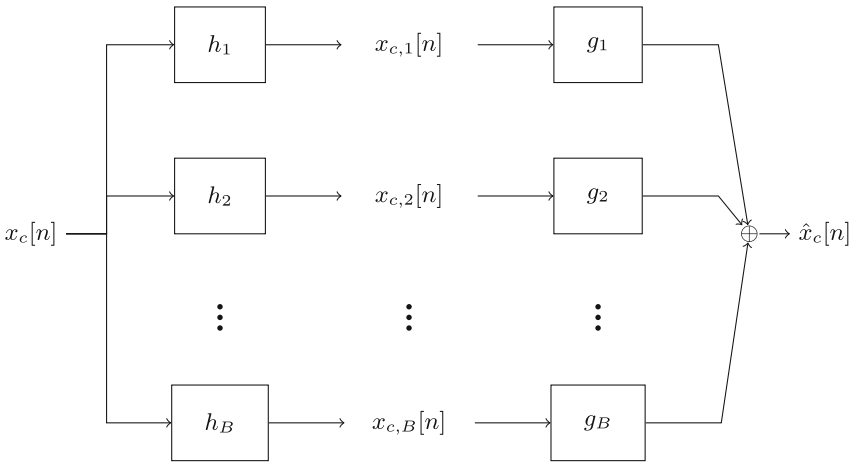

Fig. 3. The representation of filter bank analysis and synthesis. h_b and g_b represent the FIR filter to extract b^{th} frequency sub-band and the corresponding perfect reconstruction filter, respectively.

In this paper, we describe an alternative approach for artifact removal utilizing filter banks and a gating mechanism. Filter banks are an array of filters designed to decompose the signal into different components [12–14]. Although it is possible to utilize the filter banks with various types of systems, each bank is an FIR filter decomposing the signal into frequency sub-bands in the typical application, e.g. graphical equalizers. With a careful consideration on the design of the decomposition and reconstruction filters, it is possible to achieve perfect reconstruction [15]. Correspondingly, we decompose each EEG channel, $x_c[n]$ to their frequency sub-bands using filter banks with the perfect reconstruction property as in Fig. 3. As a special selection of such filters, we select h_1 to cor-

respond to a low pass filter designed in the least square sense [16] and h_b to correspond to frequency shifts of h_1.

Following the decomposition (analysis) step of the filter bank, $x_{c,b}[n]$ representing the EEG component for channel c and frequency sub-band b is obtained. Using an independent measure of artifact contamination, the temporal sections of artifacts are identified. In this paper, artifact indicator signal corresponds to eye blinks detected from an eye tracker. In non-contaminated sections, the statistics for each channel and band are learned, and in contaminated sections, the samples outside the tolerance interval of the learned statistics are removed.

The learning procedure for a single sub-band is as the following, where $o[n]$ represents a binary signal indicating the existence of artifacts:

1. Decompose each EEG channel into frequency sub-bands with a filter bank
2. $\forall$ sub-band signal $x_{c,b}[n]$ for channel c and band b and $\forall n$
   (a) If $o[n] = 0$, indicating non-contamination by artifacts, use $x_{c,b}[n]$ to estimate second order statistics of the corresponding channel and band, $\sigma_{c,b}$.
   (b) If $o[n] = 1$, indicating contamination, and $|x_{c,b}[n]| > \tau\sigma_{c,b}$, set $x_{c,b} = 0$ ($\tau = 3$)
3. Reconstruct the EEG channels, $\hat{x}_c[n]$, from modified sub-band signals, $x_{c,b}[n]$

3 Experimental Setup and Results

EEG and eye-tracker data utilized in this paper were recorded from a series of experiments designed to vary cognitive load during a set of visual psychological tasks. For most of the tasks, participants are expected to direct their gaze to various spatial elements in order to match colors, perform an n-back task and follow directional cues. Correspondingly, the nature of the tasks require frequent eye movements causing ocular artifacts in the EEG. Moreover, the most prominent components of neurophysiological activity associated with the task manipulation is expected to occur in the prefrontal cortex, which is one of the most susceptible regions to ocular artifacts.

During the sessions, EEG is acquired from a 64 channel Biosemi ActiveTwo system with the sampling rate of 256 Hz. Concurrently, pupil diameter, horizontal and vertical eye positions are recorded using an ASL EYE-TRAC 6 Series eye tracker (sampling rate: 120 Hz). Event triggers are sent to both devices through parallel port. Following an application of a linear phase high pass filter (cut-off: 1 Hz, length: 480) on the EEG to remove the low frequency drifts, the signals are synchronized and resampled to 120 Hz (sampling rate of the eye tracker). Eye tracker signals contain discontinuities due to the loss of tracking during the closure of eyes, and the selection of 120 Hz as the common sampling rate prevents distortions in the signals caused by the antialiasing filters in the resampling operation.

Using the vertical eye position from the eye tracker, eye blinks are detected via a simple thresholding on the vertical speed. A filter bank, consisting of 30 FIR filters (length 480) with 4 Hz intervals, is designed with the perfect reconstruction

property. Consequently, each EEG channel is passed through the filter bank and ocular artifacts are removed utilizing the proposed algorithm. Examples of the artifact removal for channel Fp1 are given in Fig. 4.

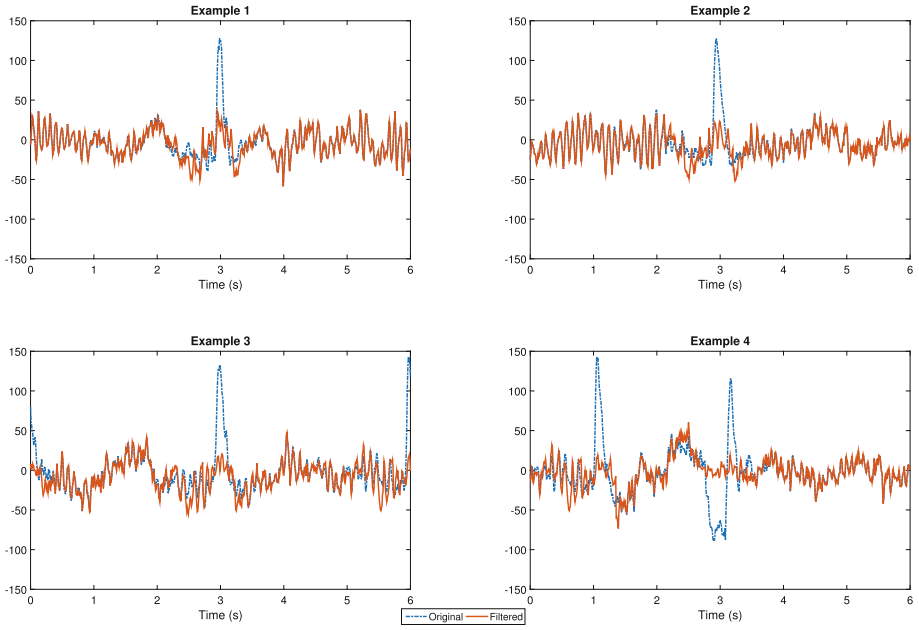

Fig. 4. Examples of artifact removal for Fp1. Proposed algorithm was also successful on effectively eliminating ocular artifacts with sporadic waveforms as in Example 4.

4 Discussion

In this paper, we demonstrated a novel methodology to filter ocular artifacts from EEG. Our approach employed filter banks in conjunction with an eye tracker based eye activity detector. The frequency sub-bands which change significantly compared to typical signal levels are removed from the temporal sections detected to be contaminated. Even though we have focused on the eye blinks in this paper, a similar methodology is applicable for other artifact sources or detectors with minor changes to this approach. For example, an accelerometer based detector may be used to remove artifacts caused by extraneous movements, or a dedicated EOG channel may be utilized for ocular artifacts. However, if different pieces of recording equipment are used as artifact detectors, a signal synchronization step, as described in Sect. 2.1, becomes imperative for alignment with EEG signals.

One of the advantages of the artifact filtering algorithm presented in this paper is that it works with a very low number of EEG channels. EEG systems with a small number of electrodes are becoming increasingly popular, as researchers begin to apply EEG-based solutions in a variety of practical tasks contexts.

While promising as an efficient and effective technique, there are several concerns associated with the proposed algorithm. First, it requires an external eye blink/artifact detector. However, widening availability of eye trackers and camera-based interaction systems (e.g. Xbox Kinect) creates a significant potential for detection of eye blink and artifact inducing events. As an alternative solution, when a camera-based detector is impractical, the difference between two frontal EEG channels with the same horizontal position may be used as an eye blink detector. Second, if the frequency content signals of interest notably overlaps with the eye blinks or changes frequently, the proposed approach may be unable to remove the artifacts without distorting the EEG.

It is possible to improve and extend the proposed algorithm in various ways. For example, setting the contaminated frequency components to zero introduces distortions at the beginning and at the end of the contaminated section. Correspondingly, a smoother transition may be achieved utilizing a window function to decrease the aggressiveness of the removal at the edges. Moreover, the detection of the level of contamination may be measured in a more probabilistic manner, as opposed to simply thresholding based on the second order statistics. Such an approach may also be used to decide on the degree of correction of contaminated samples. Furthermore, the learned statistics of the frequency sub-band may be time variant, e.g. estimated adaptively using a forgetting factor, to adapt for slow variations in the signal characteristics. Another possible track of enhancement is to utilize filter banks in a multidimensional manner with multiple EEG channels.

References

1. Mathan, S., Smart, A., Ververs, T., Feuerstein, M.: Towards an index of cognitive efficacy. In: Engineering in Medicine and Biology (2010)
2. Turner, G.R., Levine, B.: Augmented neural activity during executive control processing following diffuse axonal injury. Neurology **71**(11), 812–818 (2008)
3. Quinn, M., Mathan, S., Pavel, M.: Removal of ocular artifacts from EEG using learned templates. In: Schmorrow, D.D., Fidopiastis, C.M. (eds.) AC 2013. LNCS, vol. 8027, pp. 371–380. Springer, Heidelberg (2013)
4. Fatourechi, M., Bashashati, A., Ward, R.K., Birch, G.E.: Emg and eog artifacts in brain computer interface systems: a survey. Clin. Neurophysiol. **118**(3), 480–494 (2007)
5. Jung, T.P., Makeig, S., Westerfield, M., Townsend, J., Courchesne, E., Sejnowski, T.J.: Removal of eye activity artifacts from visual event-related potentials in normal and clinical subjects. Clin. Neurophysiol. **111**(10), 1745–1758 (2000)
6. Croft, R., Barry, R.: Removal of ocular artifact from the eeg: a review. Neurophysiol. Clin./Clin. Neurophysiol. **30**(1), 5–19 (2000)

7. Castellanos, N.P., Makarov, V.A.: Recovering eeg brain signals: artifact suppression with wavelet enhanced independent component analysis. J. Neurosci. Methods **158**(2), 300–312 (2006)
8. Gusfield, D.: Algorithms on Strings, Trees and Sequences: Computer Science and Computational Biology. Cambridge University Press, Cambridge (1997)
9. Hirschberg, D.S.: A linear space algorithm for computing maximal common subsequences. Commun. ACM **18**(6), 341–343 (1975)
10. Haykin, S.: Adaptive Filter Theory. Prentice-Hall Information and System Sciences Series. Prentice Hall, Upper Saddle River (2002)
11. Oppenheim, A., Schafer, R., Buck, J.: Discrete-Time Signal Processing. Prentice Hall International Editions. Prentice Hall, Upper Saddle River (1999)
12. Crochiere, R., Rabiner, L.: Multirate Digital Signal Processing. Prentice-Hall Signal Processing Series Advanced monographs. Prentice-Hall, Upper Saddle River (1983)
13. Cristi, R.: Modern Digital Signal Processing. Thomson/Brooks/Cole, Pacific Grove (2004)
14. Cvetkovic, Z., Vetterli, M.: Oversampled filter banks. IEEE Trans. Signal Process. **46**(5), 1245–1255 (1998)
15. Vetterli, M.: Filter banks allowing perfect reconstruction. Signal Process. **10**(3), 219–244 (1986)
16. Lim, J., Oppenheim, A.: Advanced Topics in Signal Processing. Prentice-Hall Signal Processing Series. Prentice-Hall, Upper Saddle River (1988)